

Quantum waveguides with a lateral semitransparent barrier: spectral and scattering properties

P. Exner^{a,b} and D. Krejčířik^{a,c}

a) Nuclear Physics Institute, Academy of Sciences, 25068 Řež near Prague

b) Doppler Institute, Czech Technical University, Břehová 7, 11519 Prague,

c) Faculty of Mathematics and Physics, Charles University, V Holešovičkách 2,
18000 Prague, Czech Republic

exner@ujf.cas.cz, krejcirik@ujf.cas.cz

Abstract

We consider a quantum particle in a waveguide which consists of an infinite straight Dirichlet strip divided by a thin semitransparent barrier on a line parallel to the walls which is modeled by a δ potential. We show that if the coupling strength of the latter is modified locally, *i.e.*, it reaches the same asymptotic value in both directions along the line, there is always a bound state below the bottom of the essential spectrum provided the effective coupling function is attractive in the mean. The eigenvalues and eigenfunctions, as well as the scattering matrix for energies above the threshold, are found numerically by the mode-matching technique. In particular, we discuss the rate at which the ground-state energy emerges from the continuum and properties of the nodal lines. Finally, we investigate a system with a modified geometry: an infinite cylindrical surface threaded by a homogeneous magnetic field parallel to the cylinder axis. The motion on the cylinder is again constrained by a semitransparent barrier imposed on a “seam” parallel to the axis.

1 Introduction

Quantum mechanics of constrained systems is experiencing a new wave of interest connected with the recent progress in semiconductor physics: nowadays experimentalists are able to investigate the behavior of electrons in structures of various shapes, at times rather elaborated. The small size, extreme material purity, and its crystalline structure make it possible to derive basic properties of these systems in a crude but useful model in which the electron is considered as a free particle (with an effective mass) whose motion is constrained to a prescribed subset of \mathbb{R}^d with $d = 2, 3$, possibly in presence of external fields.

On the theoretical side, this inspires questions about relations between spectral and scattering properties of such systems and the underlying geometry and topology. A class of systems which attracted a particular attention are *quantum waveguides*, *i.e.* tubular regions supporting a Schrödinger particle. It is known that a deviation from the straight tube can induce existence of bound states and resonances in scattering, vortices in probability current, *etc.*, be it bending [DE, DEM, DEŠ, EŠ, GJ]), protrusion or a similar local deformation [AS, BGRS, EV1], waveguide coupling by crossing [SRW], or by one or several lateral windows [EŠTV, EV2, EV3] (the related bibliography is rather extensive; the quoted papers contain many more references).

In this paper we are going to discuss a system closely related to the last named one. It supposes again a double waveguide; however, the coupling between the two parallel ducts will entail now a tunneling through a thin semitransparent barrier rather than a window in a hard wall separating

them — *cf.* Figure 1. To get a solvable model we describe the barrier by a δ potential whose coupling strength may vary longitudinally: the Hamiltonian can be then formally written as

$$H_\alpha = -\Delta_\Omega + \alpha(x)\delta(y) \quad (1.1)$$

with the barrier supported by the x -axis, where $\Omega := \mathbb{R} \times (-d_2, d_1)$ is the double-guide strip.

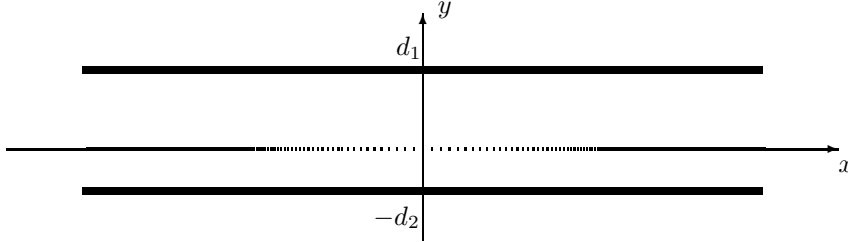


Figure 1: Double waveguide with a δ barrier.

There are several motivations to investigate a leaky-barrier waveguide pair. First of all, it is a generalization in a sense of earlier results, because the pierced-hard-wall case of Ref. [EŠTV] corresponds to $\alpha = 0$ in the window and $\alpha = \infty$ otherwise. Recall that the latter can serve to describe an actual quantum-wire coupler — see, *e.g.*, [HTW, Ku] — and such a model will certainly become more realistic if the tunneling through the barrier of a doped semiconductor material separating the two guides is taken into account. At the same time, the Hamiltonian (1.1) covers for various α a wide variety of situations.

On the mathematical side, the δ potential of (1.1) can be treated more easily than the hard-wall barrier, since two operators with different functions α have the same form domain. To illustrate the difference, one can compare the variational proof of existence of bound states in Thm 3.1 below with the analogous argument of Ref. [EŠTV]. A deeper application of the quadratic-form perturbations allows us to construct the Birman-Schwinger theory for the waveguide systems in question, in particular, to derive the weak-coupling behaviour of the bound states. This will be done in a subsequent paper [EK].

Let us describe briefly the contents of the paper. In the next section we shall describe the model and deduce its spectrum in the “unperturbed”, *i.e.* translationally invariant case. In Section 3 we demonstrate that a local change of the coupling parameter will cause the existence of bound states provided it is negative in the mean. To illustrate the spectral and also scattering properties we shall discuss then in detail the example in which the barrier function is of a “rectangular well” shape. In the final section we will show how the situation modifies if the semitransparent barrier is placed at the surface of a cylinder threaded by a homogeneous magnetic field.

2 Preliminaries

2.1 The Hamiltonian

Let $\Omega := \mathbb{R} \times \mathcal{O}$ with $\mathcal{O} := \mathcal{O}_2 \cup \mathcal{O}_1 := (-d_2, 0) \cup (0, d_1)$ be the configuration space, *i.e.*, the part of \mathbb{R}^2 occupied by the waveguide. Passing to the rational units, $\hbar = 2m = 1$, we may identify the particle Hamiltonian H_α with the Laplace operator away of the waveguide boundary and the barrier. To give meaning to the formal expression (1.1) one has to specify the boundary conditions. At the outer edges we assume the Dirichlet condition,

$$\psi(x, -d_2) = \psi(x, d_1) = 0, \quad (2.1)$$

while the barrier is transversally the usual δ potential defined conventionally as

$$\psi(x, 0+) = \psi(x, 0-) =: \psi(x, 0), \quad \psi_y(x, 0+) - \psi_y(x, 0-) = \alpha(x)\psi(x, 0) \quad (2.2)$$

for any $x \in \mathbb{R}$ — cf. [AGHH, Sec .I.3] — where the subscript denotes partial derivative with respect to y . The Hamiltonian domain is then

$$D(H_\alpha) := \{ \psi \in W_2^2(\Omega) \mid \psi \text{ satisfies (2.1) and (2.2) } \}, \quad (2.3)$$

where the function $\alpha : \mathbb{R} \rightarrow \mathbb{R}$, assumed to be piecewise continuous, determines the shape of the barrier and represents the x -dependent coupling “constant” of the interaction.

For the sake of simplicity we shall exclude the above mentioned case of a Dirichlet barrier, $\alpha(x) = \infty$ at a subset of \mathbb{R} . In that case all the operators H_α have the same form domain, and the associated quadratic form is obtained by a simple integration by parts:

$$q_\alpha[\psi] := \int_{\mathbb{R} \times \mathcal{O}} |\nabla \psi|^2(x, y) dx dy + \int_{\mathbb{R}} \alpha(x) |\psi(x, 0)|^2 dx, \quad (2.4)$$

$$D(q_\alpha) := \{ \psi \in W_2^1(\mathbb{R} \times (-d_2, d_1)) \mid \forall x \in \mathbb{R} : \psi(x, -d_2) = \psi(x, d_1) = 0 \}. \quad (2.5)$$

The form (2.4) is obviously symmetric and it is not difficult to check that it is closed and thus indeed associated with H_α . Hereafter we adopt the notation of [EŠTV]: $d := \max\{d_1, d_2\}$, $D := d_1 + d_2$, and

$$\nu := \frac{\min\{d_1, d_2\}}{\max\{d_1, d_2\}}.$$

Without loss of generality we may assume that $d_2 \leq d_1 = d$.

2.2 The unperturbed system

If $\alpha(x) = \alpha$ is a constant function, we can solve the Schrödinger equation $H_\alpha \psi = k^2 \psi$ by separation of variables. To get the transverse eigenfunctions we have to match smoothly the solutions in the two ducts, $C_2 \sin \ell(y + d_2)$ and $C_1 \sin \ell(y - d_1)$, chosen to satisfy the condition (2.1). If $\ell d_1, \ell d_2$ are not multiples of π we get thus the following condition on eigenvalues of the transverse part of the Hamiltonian:

$$-\alpha = \ell (\cot \ell d_1 + \cot \ell d_2). \quad (2.6)$$

Remark 2.1 If d_1, d_2 are rationally related the Schrödinger equation can be also solved by $\ell = \frac{\pi n p}{d_1} = \frac{\pi n q}{d_2}$, $n \in \mathbb{N} \setminus \{0\}$. However, such wave functions are zero at $y = 0$, and therefore independent of α . In this sense they represent a trivial part of the problem. A prime example is the symmetric waveguide pair, $d_1 = d_2$, where this observation concerns every solution antisymmetric w.r.t. $y = 0$. It is reasonable to concentrate on the nontrivial part only. If $\nu \equiv \frac{d_2}{d_1} = \frac{p}{q}$, we denote by \mathcal{G}_ν the subspace in $L^2(-d_2, d_1)$ spanned by the solutions of (2.6). Putting then $\mathcal{H}_\nu := L^2(\mathbb{R}) \otimes \mathcal{G}_\nu^\perp$, we shall restrict our attention to the operator $H_\alpha \upharpoonright \mathcal{H}_\nu$; for the sake of simplicity we shall denote the restriction by the symbol H_α again. The trivial part is absent, of course, if ν is irrational.

From the spectral condition (2.6) we get a sequence of eigenvalues (in the natural ascending order) of (the nontrivial part of) the transverse operator; we denote it as $\{\nu_n(\alpha)\}_{n=1}^\infty$. The corresponding eigenfunctions are

$$\chi_n(y; \alpha) = (-1)^j N_n \sin \sqrt{\nu_n} d_j \sin \sqrt{\nu_n} (y + (-1)^j d_j) \quad (2.7)$$

for $y \in \mathcal{O}_j$, $j = 1, 2$, where N_n is the normalization factor chosen in such a way that χ_n would be a unit vector in $L^2(-d_2, d_1)$, i.e.

$$N_n^2 = \frac{2\sqrt{\nu_n}}{\sqrt{\nu_n} d_1 \sin^2 \sqrt{\nu_n} d_2 + \sqrt{\nu_n} d_2 \sin^2 \sqrt{\nu_n} d_1 - \sin \sqrt{\nu_n} d_1 \sin \sqrt{\nu_n} d_2 \sin \sqrt{\nu_n} D}. \quad (2.8)$$

Furthermore, the Green’s function of the Hamiltonian (1.1) can be written down explicitly:

$$G_\alpha(x, y, x', y'; k) = \sum_{n=1}^{\infty} \frac{i}{2k_n} e^{ik_n |x - x'|} \chi_n(y; \alpha) \bar{\chi}_n(y'; \alpha), \quad (2.9)$$

where the effective momentum in the n -th transverse mode is $k_n := \sqrt{k^2 - \nu_n(\alpha)}$.

Elementary properties of the transverse eigenvalues follow from the spectral condition (2.6) by means of the implicit-function theorem; we collect them in the lemma below.

Lemma 2.2 (a) *Let $\{m_i\}_{i=0}^\infty$ be the sequence obtained from the set $\mathbb{N} \cup \nu^{-1}\mathbb{N}$ by natural ordering. Then $\frac{\pi}{2d}(n-1) \leq \frac{\pi}{d}m_{n-1} < \sqrt{\nu_n} < \frac{\pi}{d}m_n \leq \frac{\pi}{d}n$ holds for all $n \in \mathbb{N} \setminus \{0, 1\}$.*

(b) *The function $\alpha \mapsto \nu_n(\alpha)$ is strictly increasing and continuous for all $n \in \mathbb{N} \setminus \{0\}$.*

3 Existence of bound states

Depending on the choice of α , the operators (1.1) offer a variety of spectral types. In this paper we shall concentrate on the situation when the barrier describes a local perturbation of the system with separating variables considered above. The locality is at that understood as a decay of the function α ; in other words, we shall assume that $\lim_{|x| \rightarrow \infty} \alpha(x) = \alpha_0$. It is important that the limiting value α_0 is the same at both directions.

In such a case, it is easy to localize the essential spectrum. One employs a simple bracketing argument similar to that of [EŠTV, Sec. II]) squeezing H_α between a pair of operators with Dirichlet and Neumann conditions on segments perpendicular to the x -axis placed to both sides of the centre. By the minimax principle only the tails of the estimating operators contribute to their essential spectra; since the “cuts” can be chosen arbitrarily far we obtain $\sigma_{ess}(H_\alpha) = [\nu_1(\alpha_0), \infty)$.

Less trivial is the existence of discrete spectrum. It is known that any “window” in the impenetrable barrier induces a bound state. This fact was established first for sufficiently wide windows [Po], later an independent and more general proof was given [EŠTV] with no lower bound on the window width. The present case is more complicated because the effective coupling strength $\alpha - \alpha_0$ can be sign-changing. We shall show that it is sufficient if it is negative in the mean creating thus a locally average stronger tunnelling between the two channels:

Theorem 3.1 *Assume that (i) $\alpha - \alpha_0 \in L^1_{loc}(\mathbb{R})$, (ii) $\alpha(x) - \alpha_0 = \mathcal{O}(|x|^{-1-\varepsilon})$ for some $\varepsilon > 0$ as $|x| \rightarrow \infty$. If $\int_{\mathbb{R}} (\alpha(x) - \alpha_0) dx < 0$, then H_α has at least one isolated eigenvalue below its essential spectrum.*

PROOF: We use a variational argument whose idea comes back to [GJ]; see also [DE, RB], and [EŠTV, Sec. III]) for a coupled waveguide system. First of all, the assumption (ii) tells us that $\lim_{|x| \rightarrow \infty} |x|^{1+\varepsilon}(\alpha(x) - \alpha_0) = 0$, i.e., to any $\delta > 0$ there is $a_\delta > 1$ such that

$$|x| > a_\delta \Rightarrow |\alpha(x) - \alpha_0| < \frac{\delta}{|x|^{1+\varepsilon}}. \quad (3.1)$$

It is useful to introduce a shifted energy form: for an arbitrary $\Psi \in D(q_\alpha)$ we put

$$Q_\alpha[\Psi] := q_\alpha[\Psi] - \nu_1(\alpha_0)\|\Psi\|_2^2; \quad (3.2)$$

since the essential spectrum of H_α starts at $\nu_1(\alpha_0)$, we have to find a trial function Ψ such that $Q_\alpha[\Psi]$ is negative. We obtain it by a suitable modification of the function $\Psi_0(x, y) := \chi_1(y; \alpha_0)$ which formally annuls (3.2) for $\alpha = \alpha_0$ but does not belong to L^2 . The trial function has to decay; in order to make the positive contribution from its tails to the kinetic energy small, we employ an exterior scaling. We choose an interval $\mathcal{A} := [-a, a]$ for some $a > 1$ and a function $\varphi \in \mathcal{S}(\mathbb{R})$ in such a way that $\varphi(x) \leq 1$ and $\varphi(x) = 1$ on \mathcal{A} . Then we can define the family $\{\varphi_\sigma : \sigma \in \mathbb{R}\}$ by a scaling exterior to \mathcal{A} :

$$\varphi_\sigma(x) := \begin{cases} \varphi(x) & \text{if } |x| \leq a \\ \varphi(\pm a + \sigma(x \mp a)) & \text{if } \pm x > a \end{cases} \quad (3.3)$$

By construction, $|\varphi_\sigma(x)| \leq 1$ holds for all $x \in \mathbb{R}$. The sought trial function will be chosen in the form $\Psi(x, y) := \varphi_\sigma(x)\chi_1(y; \alpha_0)$. We employ the relations $\|\dot{\varphi}_\sigma\|_2^2 = \sigma\|\dot{\varphi}\|_2^2$, and

$$\begin{aligned} q_\alpha[\Psi] &= q_{\alpha_0}[\Psi] + \int_{\mathbb{R}} (\alpha(x) - \alpha_0) |\Psi(x, 0)|^2 dx, \\ q_{\alpha_0}[\Psi] &= \|\dot{\varphi}_\sigma\|_2^2 + \nu_1(\alpha_0) \|\varphi_\sigma\|_2^2, \end{aligned}$$

the last one of which is obtained by tedious but straightforward calculation. This yields

$$Q_\alpha[\Psi] = \sigma\|\dot{\varphi}\|_2^2 + |\chi_1(0; \alpha_0)|^2 \int_{\mathbb{R}} (\alpha(x) - \alpha_0) |\varphi_\sigma(x)|^2 dx. \quad (3.4)$$

We split now the integration region into two mutually disjoint parts, \mathcal{A} and $\mathbb{R} \setminus \mathcal{A}$. Using (3.1) together with the above mentioned bound on φ_σ we arrive at the estimate

$$Q_\alpha[\Psi] < \sigma\|\dot{\varphi}\|_2^2 + \frac{4\delta|\chi_1(0; \alpha_0)|^2}{\varepsilon a^\varepsilon} + |\chi_1(0; \alpha_0)|^2 \int_{\mathbb{R}} (\alpha(x) - \alpha_0) dx. \quad (3.5)$$

By assumption we have $\int_{\mathbb{R}} (\alpha(x) - \alpha_0) dx < 0$ and since $\chi_1(0; \alpha_0)$ is nonzero, the last term is negative; it is then enough to choose δ and σ sufficiently small to make $Q_\alpha[\Psi]$ negative. ■

Remark 3.2 A case of particular interest concerns weakly coupled Hamiltonian of the type (1.1), *i.e.* the situation when α differs from α_0 only slightly. In that case one can develop a Birman-Schwinger analysis in order to derive the perturbative expansion of the ground state energy in terms of a parameter measuring the “smallness” of $\alpha - \alpha_0$. This will be done in a separate paper [EK]; here we just borrow a result for a further use in this work.

There are different ways in which $\alpha - \alpha_0$ can be small. Suppose that the support of the perturbation shrinks, *i.e.* introduce $\alpha_\sigma(x) := \alpha(x/\sigma)$ with the scaling parameter $\sigma \in (0, 1]$ and consider the limit $\sigma \rightarrow 0+$. We have the following result [EK]:

Theorem 3.3 *Suppose that $\alpha - \alpha_0$ is non-zero and belongs to $L^{1+\varepsilon}(\mathbb{R}, dx) \cap L^1(\mathbb{R}, |x|^2 dx)$ for some $\varepsilon > 0$. Then H_{α_σ} has for small σ at most one simple eigenvalue $E(\sigma) < \nu_1(\alpha_0)$, and this happens if and only if $\int_{\mathbb{R}} (\alpha(x) - \alpha_0) dx \leq 0$. If this condition holds the following expansion is valid*

$$\begin{aligned} \sqrt{\nu_1 - E(\sigma)} &= -\frac{\sigma}{2} |\chi_1(0; \alpha_0)|^2 \int_{\mathbb{R}} (\alpha(x) - \alpha_0) dx \\ &+ \frac{\sigma^2}{4} |\chi_1(0; \alpha_0)|^2 \sum_{n=2}^{\infty} |\chi_n(0; \alpha_0)|^2 \int_{\mathbb{R}^2} (\alpha(x) - \alpha_0) \frac{e^{-\sigma\sqrt{\nu_n - \nu_1}|x-x'|}}{\sqrt{\nu_n - \nu_1}} (\alpha(x') - \alpha_0) dx dx' \\ &+ \mathcal{O}(\sigma^3). \end{aligned} \quad (3.6)$$

4 A “rectangular well” example

To illustrate the above result and to analyze the behaviour of coupled waveguides in more details we shall now investigate an example. We choose the barrier function α so that the corresponding Schrödinger equation can be solved numerically; this happens if α is a step-like function which makes it possible to employ the mode-matching method. The simplest nontrivial case concerns a “rectangular well” of a width $2a > 0$,

$$\alpha(x) := \begin{cases} \alpha_1 & \text{if } |x| < a \\ \alpha_0 & \text{if } |x| \leq a \end{cases}$$

for some $\alpha_1, \alpha_0 \in \mathbb{R}$. In view of Theorem 3.1 this waveguide system has bound states if and only if $\alpha_1 < \alpha_0$. In particular, one expects that in the case when $\alpha_1 = 0$ and α_0 is large positive the

spectral properties will be similar to those of the impenetrable barrier situation studied in [EŠTV]. On the other hand, the mode-matching method allows us to treat on same footing the scattering processes in our waveguide. Then there is no need to impose the above condition, because the “barrier” situation, $\alpha_1 > \alpha_0$ is expected to exhibit nontrivial scattering behaviour as well.

Henceforth, we shall denote the transverse eigenvalues in the two regions as $\nu_n^s := \nu_n(\alpha_s)$, $s := 0, 1$, $n \in \mathbb{N} \setminus \{0\}$. In view of the natural mirror symmetry with respect to the y -axis we may consider separately the symmetric and antisymmetric solutions, *i.e.* to analyze the halfstrip with the Neumann or Dirichlet boundary condition at $x = 0$, respectively. For the sake of simplicity we shall also restrict our attention to the case $\min\{\alpha_0, \alpha_1\} > \alpha_m := -(d_1^{-1} + d_2^{-1})$, when the lowest transverse eigenvalue is positive everywhere in the waveguide. The considerations presented below remain valid even without this assumption; one has just to replace the trigonometric ground-state eigenfunction for hyperbolic which makes the formulae cumbersome.

4.1 Bound states

Let us first derive an estimate which allows to localize roughly the eigenvalues. It is based on a bracketing argument similar to that used to specify the essential spectrum at the beginning of Section 3. The Hamiltonian can be squeezed between a pair of operators, $H_\alpha^{(N)} \leq H_\alpha \leq H_\alpha^{(D)}$, with additional Dirichlet/Neumann “cuts” at segments perpendicular to the waveguide axis, $x = \pm a$. The spectra of the estimating operators can be easily found and sought estimate comes from the eigenvalues of the middle part situated below ν_1^0 in combination with the minimax principle. In particular, we find that the number N of isolated eigenvalues satisfies the bounds

$$N_D + 1 \geq N \geq N_D := \left\lceil \frac{2a}{\pi} \sqrt{\nu_1^0 - \nu_1^1} \right\rceil,$$

where $\lceil \cdot \rceil$ denotes the entire part; this complements Theorem 3.1. Furthermore, the n -th eigenvalue E_n of H_α is estimated by

$$\nu_1^1 + \left(\frac{(n-1)\pi}{2a} \right)^2 \leq E_n \leq \nu_1^1 + \left(\frac{n\pi}{2a} \right)^2, \quad (4.1)$$

while the critical halfwidth a_n at which the n -th eigenvalue emerges from the continuum satisfies the bounds

$$\frac{(n-1)\pi}{2\sqrt{\nu_1^0 - \nu_1^1}} \leq a_n \leq \frac{n\pi}{2\sqrt{\nu_1^0 - \nu_1^1}}. \quad (4.2)$$

After this preliminary, let us pass to the mode-matching method. We start with the simpler case when the waveguide exhibits a mirror symmetry w.r.t. the x -axis, *i.e.* $d_1 = d_2 = d$.

4.1.1 The symmetric case

If $\nu = 1$, the Hamiltonian decouples into an orthogonal sum of the even and the odd parts, the spectrum of the latter being clearly trivial — *cf.* Remark 2.1. The two symmetries allow us to restrict ourselves to the part of Ω in the first quadrant, with Neumann or Dirichlet condition in the segment $(0, d)$ of the y -axis, and take the transverse eigenvalues determined by the spectral conditions

$$\begin{aligned} -\alpha_0 &= 2\ell \cot \ell d & \text{if } x \geq a \\ -\alpha_1 &= 2\ell \cot \ell d & \text{if } 0 \leq x < a. \end{aligned}$$

The corresponding transverse eigenfunctions are

$$\begin{aligned} \chi_n &:= -N_n^0 \sin \sqrt{\nu_n^0}(y-d) & \text{if } x \geq a, \\ \phi_n &:= -N_n^1 \sin \sqrt{\nu_n^1}(y-d) & \text{if } 0 \leq x < a, \end{aligned} \quad (4.3)$$

where N_n^s is a normalization factor chosen to make χ_n, ϕ_n unit vectors in $L^2(0, d)$, *i.e.*

$$(N_n^s)^2 = \frac{4\sqrt{\nu_n^s}}{2\sqrt{\nu_n^s}d - \sin 2\sqrt{\nu_n^s}d}. \quad (4.4)$$

The overlap integrals of elements of the two bases are easily seen to be

$$(\chi_m, \phi_n) = \frac{N_m^0 N_n^1}{\nu_m^0 - \nu_n^1} \left(\sqrt{\nu_n^1} \sin \sqrt{\nu_m^0} d \cos \sqrt{\nu_n^1} d - \sqrt{\nu_m^0} \sin \sqrt{\nu_n^1} d \cos \sqrt{\nu_m^0} \right). \quad (4.5)$$

A natural Ansatz for the solution of an energy $E \in [\nu_1^1, \nu_1^0]$ is

$$\begin{aligned} \Psi_{s/a}(x, y) &= \sum_{n=1}^{\infty} b_n^{s/a} e^{-q_n(x-a)} \chi_n(y) && \text{for } x \geq a \\ \Psi_{s/a}(x, y) &= \sum_{n=1}^{\infty} a_n^{s/a} \left\{ \begin{array}{l} \frac{\cosh p_n x}{\cosh p_n a} \\ \frac{\sinh p_n x}{\sinh p_n a} \end{array} \right\} \phi_n(y) && \text{for } 0 \leq x < a \end{aligned} \quad (4.6)$$

where the subscripts (we will omit them for the most part) s, a distinguish the symmetric and antisymmetric case, respectively. The longitudinal momenta are defined by

$$q_n := \sqrt{\nu_n^0 - E}, \quad p_n := \sqrt{\nu_n^1 - E}.$$

As an element of the domain (2.3), the function Ψ should be continuous together with its normal derivative at the segment dividing the two regions, $x = a$. Using the orthonormality of $\{\chi_n\}$ we get from the requirement of continuity

$$b_m = \sum_{n=1}^{\infty} a_n (\chi_m, \phi_n). \quad (4.7)$$

In the same way, the normal-derivative continuity at $x = a$ yields

$$b_m q_m + \sum_{n=1}^{\infty} a_n p_n \left\{ \begin{array}{l} \tanh \\ \coth \end{array} \right\} (p_n a) (\chi_m, \phi_n) = 0. \quad (4.8)$$

Substituting from (4.7) to (4.8), we can rewrite it as an operator equation

$$\mathbf{C} \mathbf{a} = \mathbf{0}, \quad (4.9)$$

where

$$C_{mn} := \left(q_m + p_n \left\{ \begin{array}{l} \tanh \\ \coth \end{array} \right\} (p_n a) \right) (\chi_m, \phi_n) \quad (4.10)$$

with the overlap integrals given by (4.5).

It is straightforward to compute the norms of the functions (4.6); since $n^{-1}q_n$ and $n^{-1}p_n$ tend to $\frac{\pi}{d}$ as $n \rightarrow \infty$ (see Lemma 2.2 1.), the square integrability of Ψ requires the sequences $\{a_n\}$ and $\{b_n\}$ to belong to the space $\ell^2(n^{-1})$.

To make sure that the equation (4.9) makes sense, it is enough to notice that if Ψ is an eigenvector of H_α , it must belong to the domain of any integer power of this operator. It is easy to check that

$$\forall i \in \mathbb{N} \setminus \{0\} : \quad \Psi \in D(H_\alpha^i) \Leftrightarrow \{a_n\}, \{b_n\} \in \ell^2(n^{4i-1}); \quad (4.11)$$

hence the sought sequences should belong to $\ell^2(n^r)$ for all $r \geq -1$, *i.e.* both sequences have a faster than powerlike decay. This fact also justifies *a posteriori* the interchange of summation and differentiation we have made in the matching procedure. Furthermore, one can use it to check the existence of a convergent series of cut-off approximants to the solutions in the same way as in [EŠTV, Sec. IV.1].

Remark 4.1 (an alternative method) We can use the orthonormality of $\{\phi_n\}$ instead of $\{\chi_n\}$ and express $\{a_n\}$ in analogy to (4.7), and then substitute it into (4.8). We find that the coefficient sequence $\{b_n\}$ is then determined by the following equation:

$$\mathbf{b} + \mathbf{K}\mathbf{b} = \mathbf{0}, \quad (4.12)$$

where

$$K_{mn} := \frac{1}{q_m} \sum_{k=1}^{\infty} (\chi_m, \phi_k) p_k \left\{ \begin{array}{l} \tanh \\ \coth \end{array} \right\} (p_k a) (\phi_k, \phi_n). \quad (4.13)$$

The two approaches (4.9), (4.12) are, of course, equivalent, however, it may be useful to combine them in order to get a good idea about the numerical stability of the solution. For instance, in the situation of [ESTV] the approximants of (4.9) approach the limiting values from above, while those referring to (4.12) are increasing.

4.1.2 The Asymmetric Case

Let us pass now to the case, when the widths of the ducts are nonequal, $\nu \neq 1$. In view of the mirror symmetry, we shall consider right-halfplane part of Ω only with the Neumann and Dirichlet condition on the segment $[-d_2, d_1]$ of the y -axis. The asymmetric case differs from the previous one just in the choice of transverse basis: now we can take

$$\begin{aligned} \chi_n(y) &:= \chi_n(y; \alpha_0) & \text{if } x \geq a \\ \phi_n(y) &:= \chi_n(y; \alpha_1) & \text{if } 0 \leq x < a, \end{aligned} \quad (4.14)$$

where $\chi_n(\cdot, \alpha_s)$ are of the form (2.7) with the norms N_n^s given by (2.8). The corresponding eigenvalues ν_n^0, ν_n^1 are then determined by

$$\begin{aligned} -\alpha_0 &= \ell (\cot \ell d_1 + \cot \ell d_2) & \text{if } x \geq a \\ -\alpha_1 &= \ell (\cot \ell d_1 + \cot \ell d_2) & \text{if } 0 \leq x < a. \end{aligned}$$

(see (2.6)) and the overlap integrals are

$$\begin{aligned} (\chi_m, \phi_n) &= \frac{N_m^0 N_n^1}{\nu_m^0 - \nu_n^1} \left(\sqrt{\nu_n^1} \sin \sqrt{\nu_m^0} d_1 \sin \sqrt{\nu_m^0} d_2 \sin \sqrt{\nu_n^1} D \right. \\ &\quad \left. - \sqrt{\nu_m^0} \sin \sqrt{\nu_n^1} d_1, \sin \sqrt{\nu_n^1} d_2 \sin \sqrt{\nu_m^0} D \right). \end{aligned} \quad (4.15)$$

The rest of the argument does not change and one has again to solve the equation (4.9) (respectively, (4.12)). By a straightforward modification of the above argument, one can also check that the coefficient sequences have a faster than powerlike decay and that the equation can be solved by a sequence of truncations.

4.2 Scattering

As we said in the opening of this section, the scattering can be treated in an analogous way. The incident wave is supposed to be of the form $e^{-ik_r x} \chi_r(y; \alpha_0)$, *i.e.*, to come from the right in the r -th transverse mode; we have introduced the effective momentum $k_r := \sqrt{k^2 - \nu_r^0}$. We denote by r_{rn}, t_{rn} , respectively, the corresponding reflection and transmission amplitudes to the n -th transverse mode. Due to the mirror symmetry, we can again separate the symmetric and antisymmetric situation w.r.t. $x = 0$ and to write

$$r_{rn} = \frac{1}{2}(\rho_{rn}^s + \rho_{rn}^a), \quad t_{rn} = \frac{1}{2}(\rho_{rn}^s - \rho_{rn}^a), \quad (4.16)$$

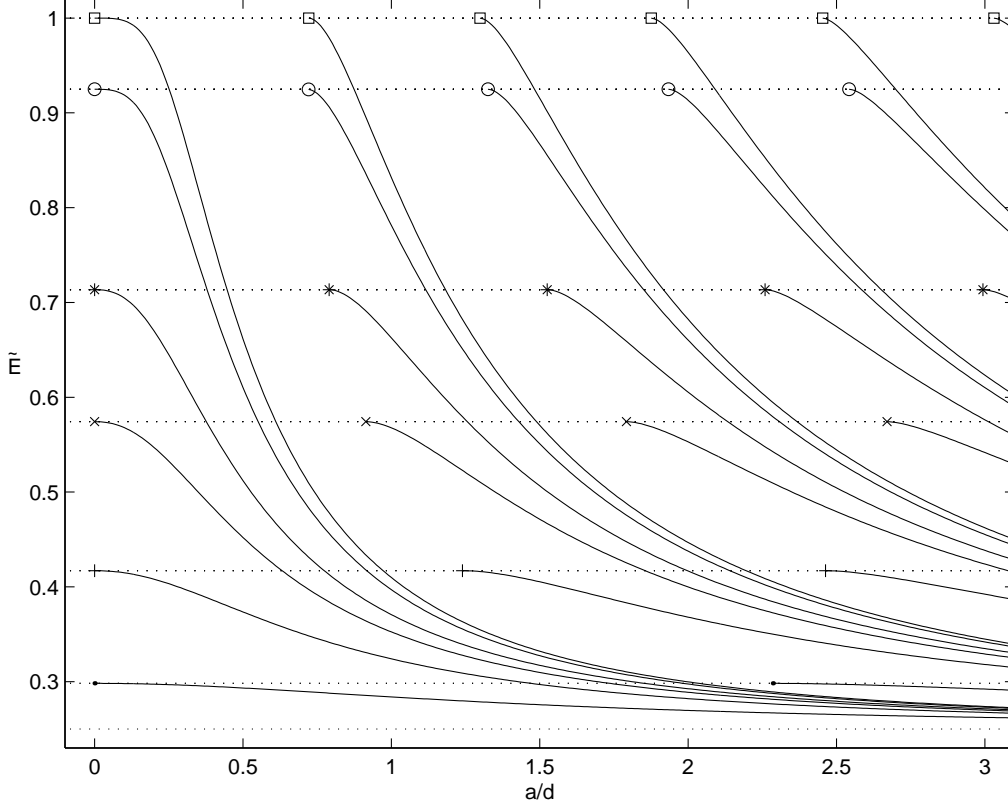


Figure 2: Bound state energies *vs.* the halfwidth \tilde{a} in the symmetric case for $\tilde{\alpha}_0 = 10^5$ (\square), 50 (\circ), 10 ($*$), 5 (\times), 2 ($+$), 0.5 (\bullet).

where ρ_{rn}^σ , $\sigma = s, a$, are the reflection amplitudes in a half of our waveguide with the Neumann and Dirichlet condition at $x = 0$, respectively. We use the following Ansatz

$$\begin{aligned} \Psi_{s/a}(x, y) &= \sum_{n=1}^{\infty} \left(\delta_{rn} e^{-ik_n(x-a)} + \rho_{rn}^{s/a} e^{ik_n(x-a)} \right) \chi_n(y) \quad \text{for } x \geq a \\ \Psi_{s/a}(x, y) &= \sum_{n=1}^{\infty} a_n^{s/a} \left\{ \begin{array}{l} \frac{\cos p_n x}{\cos p_n a} \\ \frac{\sin p_n x}{\sin p_n a} \end{array} \right\} \phi_n(y) \quad \text{for } 0 \leq x < a \end{aligned} \quad (4.17)$$

for the total energy k^2 of the incident wave in the r -th mode. The quantities $p_n := \sqrt{k^2 - \nu_n^2}$ are effective momenta in the “interaction” region. Matching these functions smoothly at $x = a$ we arrive in the same way as above at the equation

$$C a = f, \quad (4.18)$$

where

$$C_{mn} := \left(ik_m + p_n \left\{ \begin{array}{l} \tan \\ -\cot \end{array} \right\} (p_n a) \right) (\chi_m, \phi_n) \quad (4.19)$$

$$f_m := 2ik_m \delta_{rm}, \quad (4.20)$$

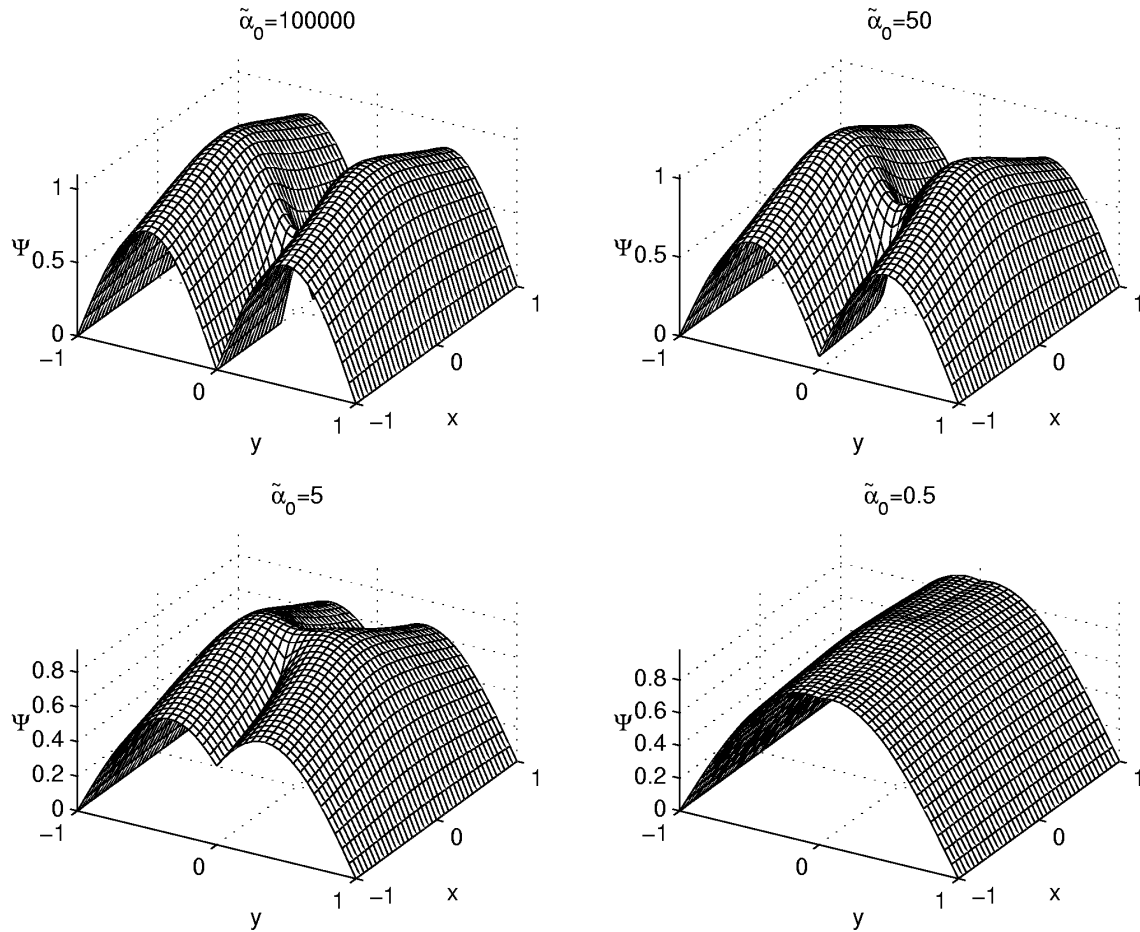


Figure 3: Ground-state eigenfunctions in the symmetric case for $a/d = 0.15$.

where the index r corresponds to the incident wave and the overlap integrals are given again by (4.15). The reflection amplitudes are then given by

$$\rho_{rm} = -\delta_{rm} + \sum_{n=1}^{\infty} a_n(\chi_m, \phi_n); \quad (4.21)$$

they determine the full S-matrix via (4.16). A quantity of direct physical interest is rather the conductivity given by the Landauer formula. If we express it in the standard units $2e^2/h$, it equals

$$G(k) = \sum_{m,n=1}^{[k]} \frac{k_n}{k_m} |t_{mn}(k)|^2, \quad (4.22)$$

where $t_{mn}(k)$ are the coefficients (4.16). The summation runs over all open channels. Another physically interesting quantity is the probability flow distribution associated with the generalized eigenvector $\Psi = \Psi_s + \Psi_a$, which is defined in the standard way,

$$\vec{j}(\vec{x}) = 2 \operatorname{Im} (\bar{\Psi}(\vec{x}) \nabla \Psi(\vec{x})). \quad (4.23)$$

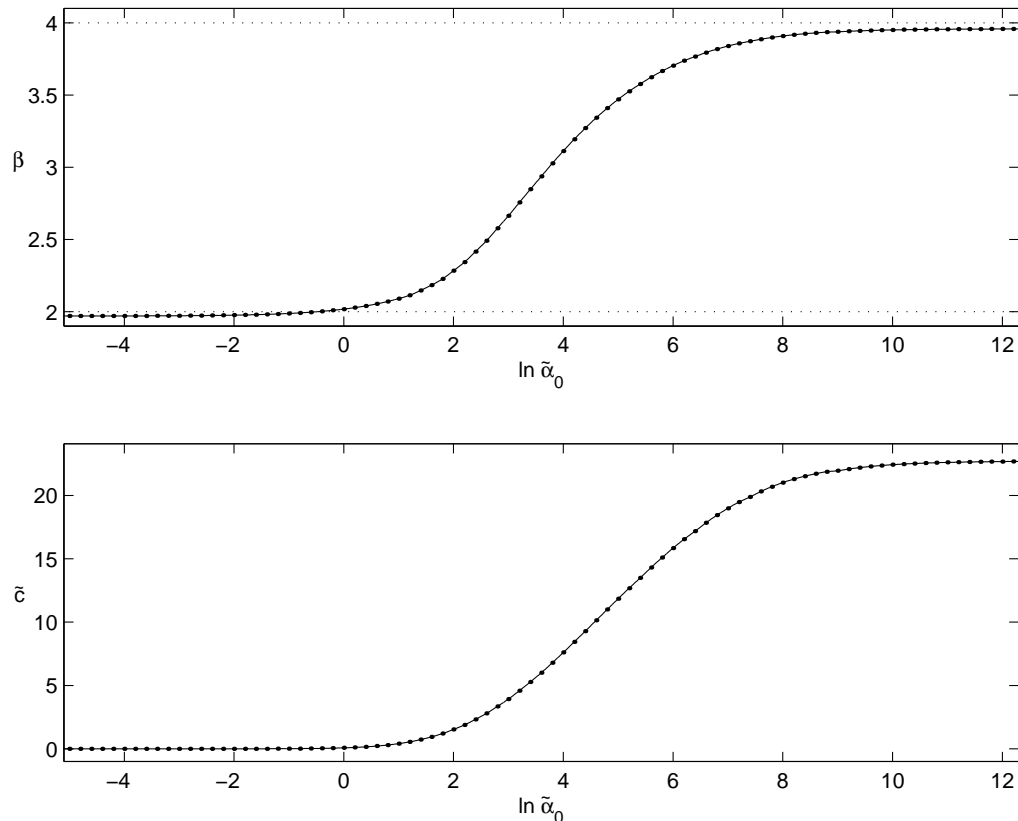


Figure 4: Narrow-window asymptotic power and coefficient as functions of α_0 .

4.3 Numerical results

Since the spectrum behaves naturally at scaling transformations it is reasonable to solve the equations (4.9) and (4.18) in the natural non-dimensional quantities. We mark them by tilde and use them to label the axis in the figures, *e.g.*, $a = d\tilde{a}$, $\alpha_s = \tilde{\alpha}_s/d$, $E = (\pi/d)^2\tilde{E}$ or $k = (\pi/d)\tilde{k}$.

4.3.1 Bound states

Eigenvalues: Figure 2 shows the bound-state energies as functions of the “window” halfwidth a for an “empty window”, $\alpha_1 = 0$. Several curves referring to different values of the barrier coupling constant α_0 are plotted. In accordance with the general results of Section 4.1 the energies decrease monotonously with the increasing “window” width and one can sandwich them between the estimates (4.1). We also see that for a fixed a the energies increase with respect to α_0 and ν ; recall that their number increases as a function of α_0 but it decreases as the waveguide becomes more asymmetric — these facts are clear from (4.1), (4.2), and Lemma 2.2. It is illustrative to confront our results for large α_0 with the energies computed in [EŠTV] for the case which corresponds formally to $\alpha_0 = \infty$. Comparing Figure 2 with Fig. 2 of the mentioned paper we see that our result for $\tilde{\alpha}_0 = 10^5$ is practically identical with the latter.

Eigenfunctions: The evolution of the ground-state wavefunction with respect to α_0 for an empty window of the fixed halfwidth $\tilde{a} = 0.15$ is illustrated on Figure 3. If the barrier tunneling is

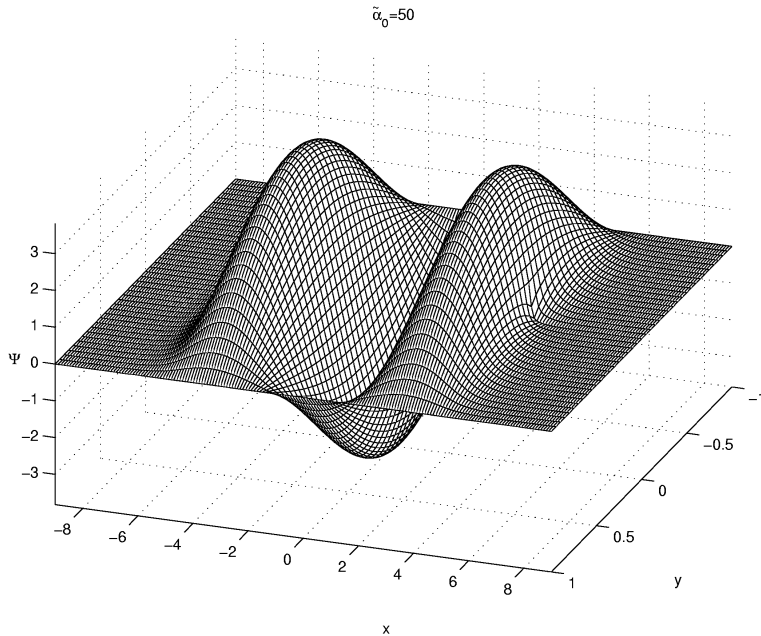


Figure 5: The eigenfunction of the second excited state for $\nu = 1$, $a/d = 5$, $\alpha_1 = 0$.

negligible, $\tilde{\alpha}_0 = 10^5$, the picture is indistinguishable from Fig. 3 in [EŠTV]. As α_0 becomes smaller we see how the wavefunction part penetrating the barrier grows.

Threshold behaviour: Consider again the empty-window case, $\alpha_1 = 0$. As a consequence of Theorem 3.3 we get for the ground-state energy for any fixed α_0 and a narrow window the asymptotic formula (*cf.* (3.6))

$$E(a) = \nu_1^0 - c a^2 + \mathcal{O}(a^3), \quad c := a^2 \alpha_0^2 |\chi_1(0; \alpha_0)|^4. \quad (4.24)$$

On the other hand, in the case of a window in the Dirichlet barrier, $\alpha_0 = \infty$, it was conjectured in [EŠTV] that we may suppose

$$E(a) = \left(\frac{\pi}{d}\right)^2 - C(\nu) a^4 + \mathcal{O}(a^5) \quad (4.25)$$

as $a \rightarrow 0+$. The conjecture is supported by a two-sided asymptotic estimate [EV2]: there are positive c_1, c_2 such that

$$-c_1 a^4 \leq E(a) - \left(\frac{\pi}{d}\right)^2 \leq -c_2 a^4$$

(for a generalization of this result to a larger number of windows and higher dimensions see [EV3]). Quite recently, a proof of (4.25) has been proposed by Popov [Pop].

This seems to be a paradox. In order to make sense of these considerations, we suppose that $E(a) = \nu_1^0 - c a^\beta$ for small a of an interval $0.016 < \tilde{a} < \tilde{a}_{max}$ ($\tilde{a}_{max} = \tilde{a}_{max}(\alpha_0)$ is chosen in such a way to include the best correlated points), and investigate numerically the dependence of the coefficients β and c ($\tilde{c} = d^{\beta+2} c / \pi^2$) on α_0 . The powerlike asymptotic behaviour is confirmed when we redraw the first eigenvalue curves of Figure 2 in the logarithmic scale. The obtained dependence of the coefficients on α_0 in the symmetric case $\nu = 1$, is illustrated on Figure 4. We see that the power reaches the values $\beta = 2, 4$ for small and large α_0 , respectively (a slight shift in the first graph is due the truncation; the convergence becomes very slow for small a). At the same time, the numerically found c for small α_0 coincides with that of (4.24).

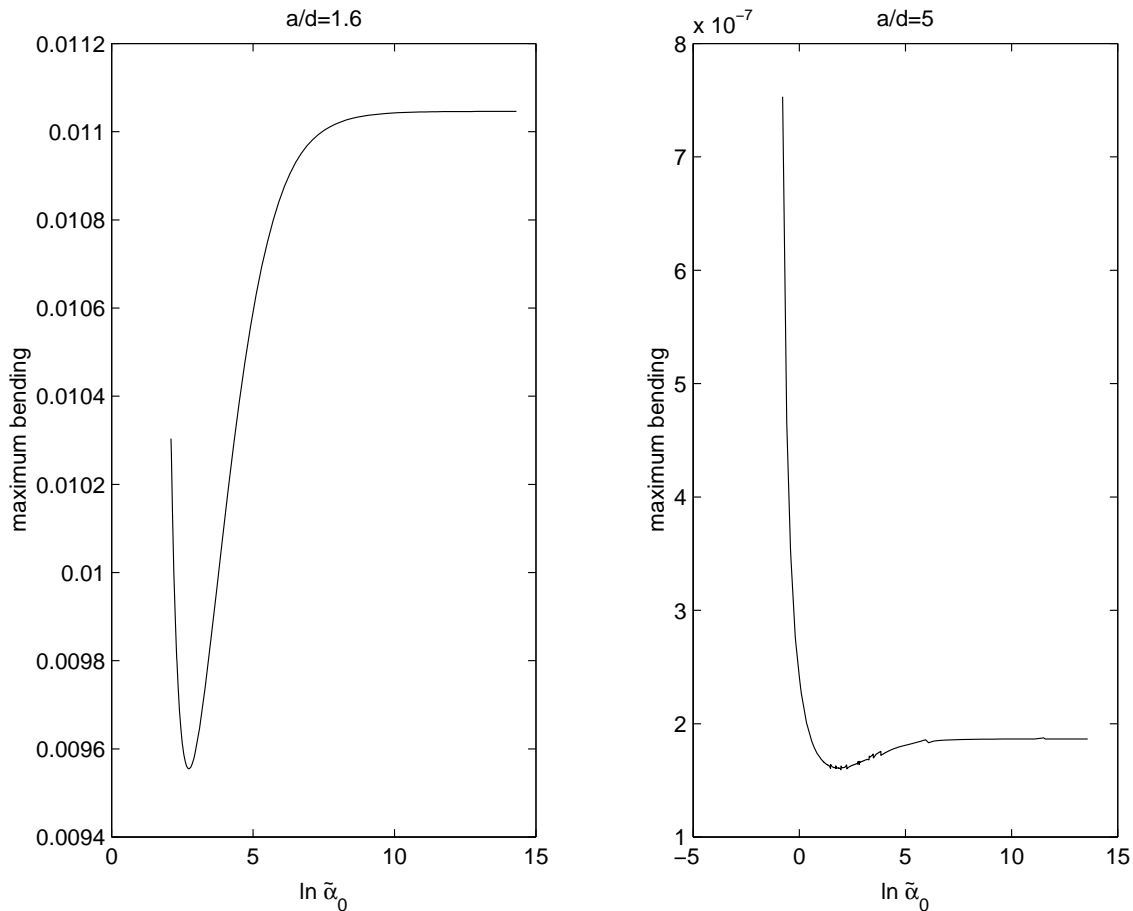


Figure 6: The maximum bending of nodal lines of third eigenfunctions in the symmetric case as a function of α_0 for a fixed window width.

Of course, the asymptotical behaviour is governed by (4.24) for any finite α_0 . The above result says only that the transition from biquadratic to quadratic asymptotics occurs for large α_0 at values of a still smaller than those we have used.

Nodal Lines: In Figure 5 we plot the third eigenfunction. Its nodal lines are almost straight showing thus that the “spikes” at the window edges act almost as a hard barrier. On the other hand, a simple argument based on the reflection principle shows that the nodal lines cannot be straight. Closer inspection shows that they have the form of a bow bent outward. The maximum bending is shown on Figure 6. It decreases rapidly with the window width which confirms the tunneling nature of the effect. Nodal lines of higher eigenfunctions exhibit (as functions of α_0) irregularities connected with the changes in the number of the modes.

4.3.2 Scattering

Conductivity: Figure 7 illustrates the evolution of the conductivity for the particle coming from the right and leaving to the left as a function of the momentum k and the width d_2 . We see that the perturbation, $-\alpha_0$ in the window, deforms the ideal steplike shape with jumps at transverse thresholds; deep resonances are clearly visible. For an almost impenetrable barrier, $\tilde{\alpha}_0 = 10^5$, we practically reproduce Fig. 5a of [EŠTV].

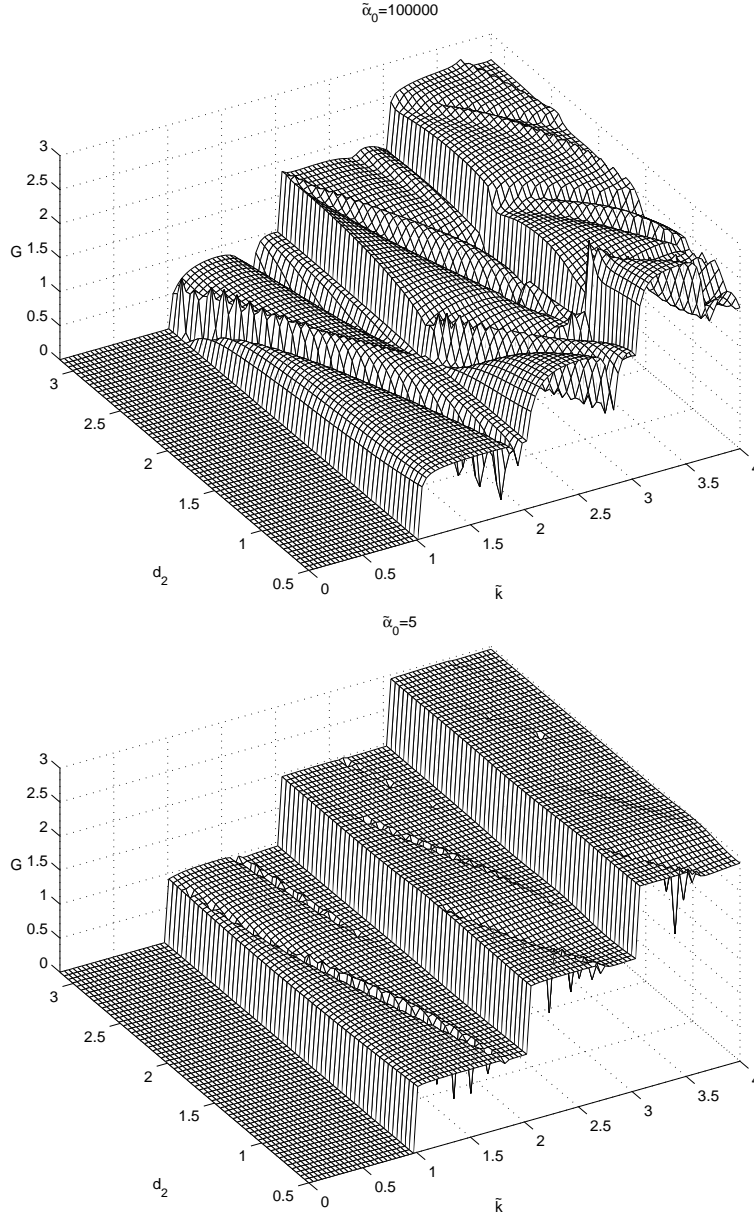


Figure 7: Right-left conductivity as a function of k , d_2 for $d = \pi$, $a = 2\pi$, $\alpha_1 = 0$.

Probability flow: Examples of the quantum probability flow are shown on Figure 8. The flow patterns change with the momentum of the incident particle and the value of α_0 . They exhibit conspicuous vortices at the resonance energies which correspond to the “trapped part” of the wavefunction. An interesting phenomenon is illustrated on the first two graphs of Figure 8: for $\tilde{\alpha}_0 = 10^5$ there is a double vortex (corresponding to the sharp stopping resonance of Figure 7), right-handed in the upper duct, while for $\tilde{\alpha}_0 = 50$ we get a left-handed vortex. The conductivity is small in these situations so the waveguide system is effectively closed for the particle transport. As α_0 decreases the conductivity grows and the waveguide opens — *cf.* Figure 8 for $\tilde{\alpha}_0 = 10, 2$.

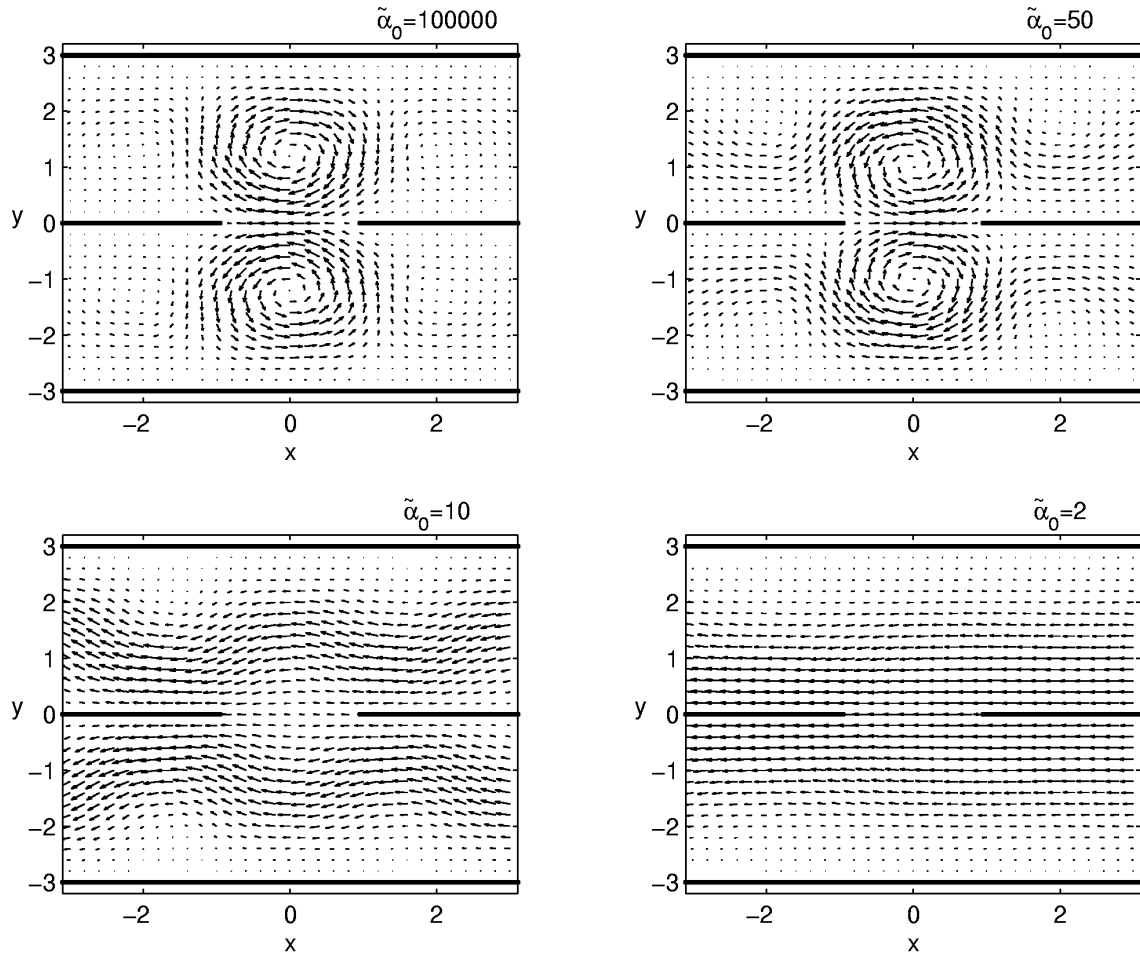


Figure 8: Probability flow patterns for $\tilde{k} = 1.745$ and $\alpha_1 = 0$ in the symmetric situation.

5 An Aharonov-Bohm cylinder

In the closing section we want to show now how the preceding considerations modify for a different geometry: we consider a nonrelativistic quantum particle living on the surface of an infinite straight cylinder of a radius R , which is threaded by a homogeneous magnetic field \vec{B} parallel to the cylinder axis. We assume that the motion is further restricted by a δ -barrier supported by a line parallel to the axis.

5.1 General considerations

The configuration space is sketched on Figure 9 where we indicate also how the coordinate system is chosen. In these coordinates we have

$$\tilde{\Omega} := \{(x, y, z) \in \mathbb{R}^3 \mid y^2 + z^2 = R^2\}. \quad (5.1)$$

Choosing the gauge so that the electromagnetic potentials fulfill $\varphi(\vec{x}) \equiv 0$ and $\vec{A}(\vec{x}) = \frac{1}{2}\vec{B} \times \vec{x}$, the Hamiltonian acquires the form

$$\tilde{H}_\alpha := (-i\nabla + \vec{A})^2 = -\Delta - i\frac{B}{2}(y\partial_z - z\partial_y) + \frac{B^2 R^2}{4} \quad (5.2)$$

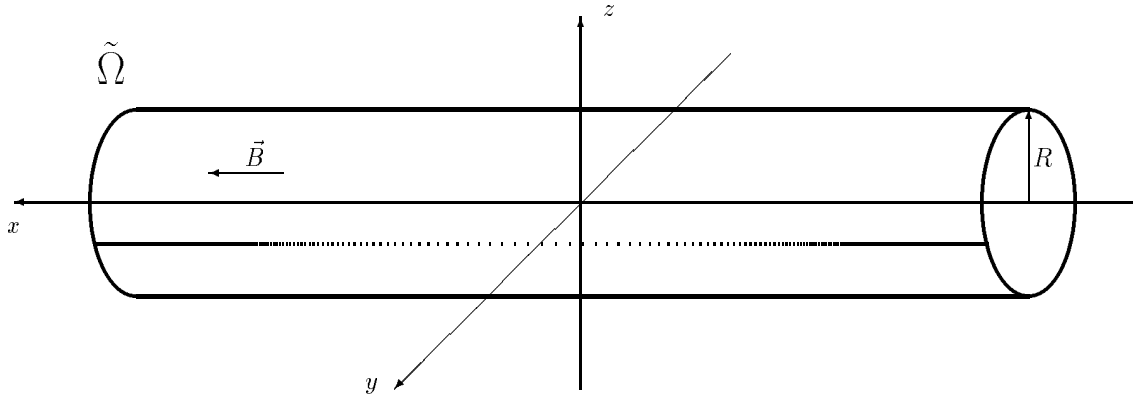


Figure 9: Cylindrical strip with a δ barrier in axial magnetic field.

away of the barrier, where $B := |\vec{B}|$; as before we put $\hbar = 2m = 1$, and also $e = -1$ having in mind an electron. The subscript α indicates the real function which defines the shape of the barrier as in the strip waveguide situation; it will enter the boundary condition (5.4) below. The vector potential has obviously the angular component $A_\varphi \equiv A$ and it equals

$$A = \frac{1}{2}BR = \frac{\phi}{2\pi R}, \quad (5.3)$$

where ϕ is the magnetic flux through the cylinder. Recall that in the rational units we use here, the natural unit of the magnetic flux is $\phi_0 := (2\pi)^{-1}$. Since we deal with a quantum system living on a surface it is natural to “unfold” it and to study (5.2) on a planar strip with appropriate boundary conditions, namely

$$\psi(u, 0+) = \psi(u, 2\pi R-) =: \psi(u, 0), \quad \psi_v(u, 0+) - \psi_v(u, 2\pi R-) = \alpha(u)\psi(u, 0), \quad (5.4)$$

where the subscript denotes again a partial derivative. To this aim, we introduce the unitary transformation $U : L^2(\tilde{\Omega}) \rightarrow L^2(\mathbb{R} \times [0, 2\pi R])$, $dudv$ by

$$(U\psi)(u, v) := \psi(u, R \cos \frac{v}{R}, R \sin \frac{v}{R}), \quad (5.5)$$

which maps $\tilde{\Omega}$ onto the strip $\Omega := \mathbb{R} \times [0, 2\pi R]$; the operator \tilde{H}_α is then unitarily equivalent to

$$H_\alpha := U\tilde{H}_\alpha U^{-1} = -\partial_u^2 + (-i\partial_v + A)^2, \quad (5.6)$$

with the domain

$$D(H_\alpha) := \{ \psi \in W_2^2(\Omega) \mid \forall u \in \mathbb{R} : \text{b.c. (5.4) are satisfied} \}. \quad (5.7)$$

We will need also the quadratic form q_α associated with H_α . Its domain is $D(q_\alpha) := W_2^1(\Omega)$ and

$$\begin{aligned} q_\alpha[\psi] &:= \int_\Omega |\nabla\psi|^2(u, v) dudv + \int_\mathbb{R} \alpha(u) |\psi(u, 0)|^2 du \\ &\quad - 2iA \int_\Omega (\bar{\psi}\partial_v\psi)(u, v) dudv + A^2 \int_\Omega |\psi|^2(u, v) dudv. \end{aligned} \quad (5.8)$$

As a comparison operator we employ again the one with $\alpha(u) = \alpha = \text{const}$ when we can solve the Schrödinger equation by separation of variables. We denote by $\{\nu_n\}_{n=1}^\infty$ and $\{\chi_n\}_{n=1}^\infty$ the (properly ordered) sequences of the transverse eigenvalues and the corresponding eigenfunctions,

respectively. Since our system is now more complicated due to the presence of the magnetic field, we have to distinguish several possibilities:

1. No barrier, $\alpha = 0$:

$$\forall \ell \in \mathbb{Z} : \quad \tilde{\chi}_\ell(v) = \frac{1}{\sqrt{2\pi R}} e^{i\frac{\ell}{R}v}. \quad (5.9)$$

The tilde marks the eigenfunctions corresponding to the eigenvalues $(\frac{\ell}{R} + A)^2$; to get $\{\nu_n\}$ one has to arrange these latter into an ascending sequence. The respective eigenfunctions will be then denoted as $\{\chi_n\}$.

2. $\alpha \neq 0$ and $2RA \notin \mathbb{N}$:

$$\forall n \in \mathbb{N} \setminus \{0\} : \quad \chi_n(v) = N_n e^{-iAv} \left(e^{i\sqrt{\nu_n}v} - \frac{e^{i2\pi RA} - e^{i2\pi R\sqrt{\nu_n}}}{e^{i2\pi RA} - e^{-i2\pi R\sqrt{\nu_n}}} e^{-i\sqrt{\nu_n}v} \right), \quad (5.10)$$

where N_n denotes the normalization factor chosen to make χ_n a unit vector in $L^2(0, 2\pi R)$,

$$|N_n|^2 := \frac{\sqrt{\nu_n} [1 - \cos 2\pi R(\sqrt{\nu_n} + A)]}{4\pi R \sqrt{\nu_n} (1 - \cos 2\pi RA \cos 2\pi R\sqrt{\nu_n}) + 2 \sin 2\pi R\sqrt{\nu_n} (\cos 2\pi RA - \cos 2\pi R\sqrt{\nu_n})}, \quad (5.11)$$

and the increasing sequence $\{\nu_n\}$ arises from the spectral condition

$$-\alpha = 2\ell \left(\cot 2\pi R\ell - \frac{\cos 2\pi RA}{\sin 2\pi R\ell} \right). \quad (5.12)$$

In analogy with Lemma 2.2(a) we have $\sqrt{\nu_n} \in \frac{1}{2R}(n-1, n)$ for any $n \in \mathbb{N} \setminus \{0\}$.

3. $\alpha \neq 0$ and integer flux, $2RA \in 2\mathbb{N}$:

The transverse eigenfunctions are of the form (5.10), while the spectral condition (5.12) changes to

$$\alpha = 2\ell \tan \pi R\ell. \quad (5.13)$$

Moreover, for $\ell \in \frac{1}{R}\mathbb{N}$ we always get the trivial solutions

$$\chi_n^{triv}(v) = \frac{1}{\sqrt{\pi R}} e^{-iAv} \sin \ell v, \quad (5.14)$$

which are independent of α . The roots $\{\tilde{\nu}_n\}$ of (5.13) satisfy the estimates $\sqrt{\tilde{\nu}_1} \in \frac{1}{2R}(0, 1)$ and $\sqrt{\tilde{\nu}_n} \in \frac{1}{2R}(2n-3, 2n-1)$ for $n \in \mathbb{N} \setminus \{0, 1\}$.

4. $\alpha \neq 0$ and half-integer flux, $2RA \in 2\mathbb{N} + 1$:

As in the two preceding cases the transverse eigenfunctions are still (5.10) but the spectral condition (5.12) changes now to

$$-\alpha = 2\ell \cot \pi R\ell. \quad (5.15)$$

The wave functions of the trivial solutions, $\ell \in \frac{1}{2R}(2\mathbb{N} + 1)$ are (5.14) again and the nontrivial roots of (5.15) satisfy $\sqrt{\tilde{\nu}_n} \in \frac{1}{2R}(2n-2, 2n)$ for all $n \in \mathbb{N} \setminus \{0\}$.

Remark 5.1 The integer and half-integer values here refer to the natural flux unit mentioned above. The essential instrument for proving the existence of bound states is the requirement $\chi_1(0) \neq 0$ (compare, *e.g.*, to Eq. (3.4) above). In the absence of a barrier, $\alpha = 0$, the eigenfunctions are always positive (see (5.9)) and $\chi_1(0) \neq 0$ holds for $\alpha \leq \alpha_m := -\frac{2\sin^2 \pi RA}{\pi R}$. In the case of a (half-)integer flux we have to exclude the trivial solutions (5.14). It is an analogy of the trivial-part exclusion described in Remark 2.1; the difference is that the triviality now does not come from the waveguide geometry, but rather from the magnetic field, *i.e.*, an external parameter. It is also clear that the ground-state eigenfunction of the class (5.10) can vanish at the barrier only if $\alpha > 0$ and the flux is half-integer.

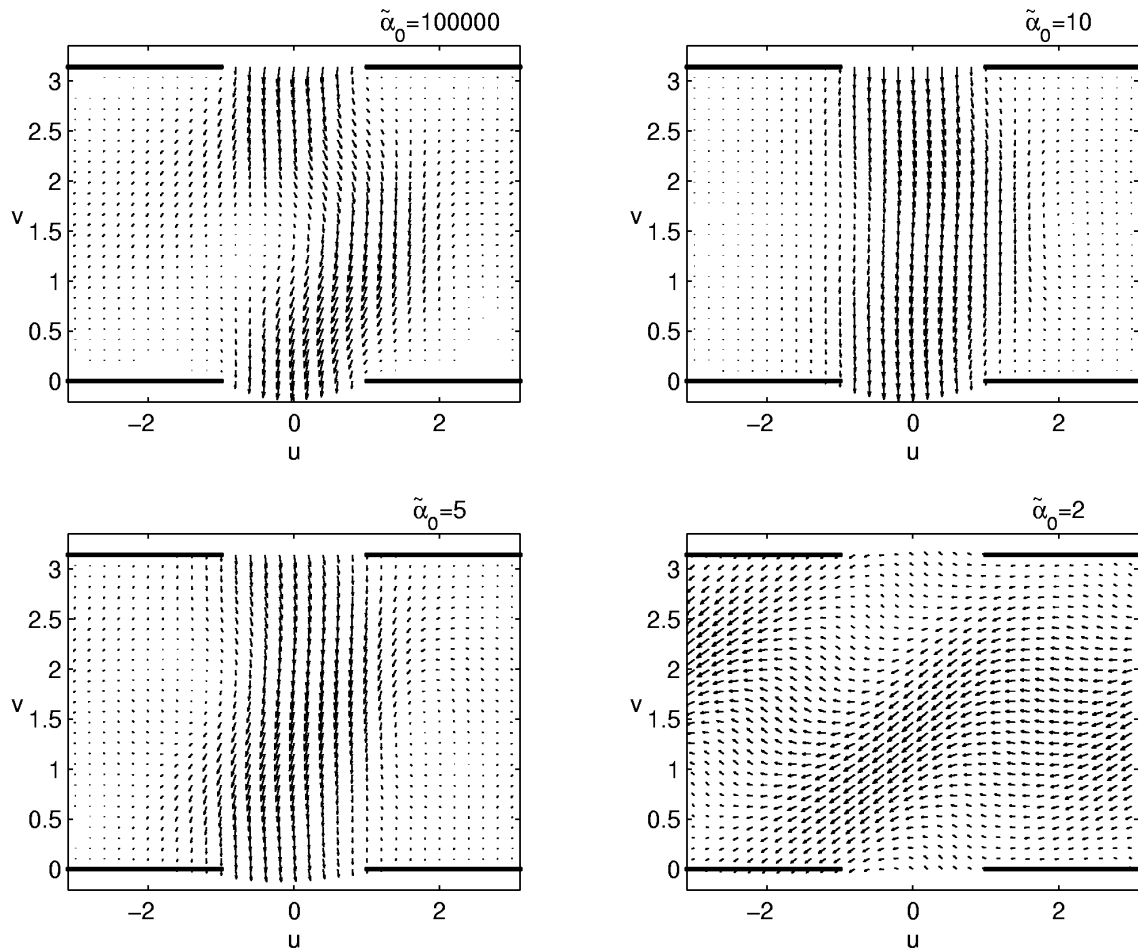


Figure 10: The quantum probability flow on the cylinder surface for $\tilde{A} = 0.5$, $\tilde{k} = 1.705$ and $\tilde{\alpha}_1 = 10^{-5}$.

5.2 An example

We shall illustrate the above consideration on a “rectangular-well” example analogous to that of Section 4. Most of the argument proceeds as there, one has just to use the different eigenfunctions and to recompute for them the overlap integrals:

$$\begin{aligned}
 (\chi_m, \phi_n) &= \frac{8 \bar{N}_m^0 N_n^1}{(e^{-i2\pi RA} - e^{i2\pi R\sqrt{\nu_m^0}})(e^{i2\pi RA} - e^{-i2\pi R\sqrt{\nu_n^1}})(\nu_m^0 - \nu_n^1)} \cdot \\
 &\cdot \left[\sqrt{\nu_m^0} \sin 2\pi R\sqrt{\nu_n^1} (\cos 2\pi RA - \cos 2\pi R\sqrt{\nu_m^0}) \right. \\
 &\quad \left. - \sqrt{\nu_n^1} \sin 2\pi R\sqrt{\nu_m^0} (\cos 2\pi RA - \cos 2\pi R\sqrt{\nu_n^1}) \right] \quad (5.16)
 \end{aligned}$$

for $\alpha_0 \neq 0 \neq \alpha_1$ with $m, n \in \mathbb{N} \setminus \{0\}$, and

$$(\chi_m, \phi_\ell) = \frac{4 \bar{N}_m^0 \sqrt{\nu_m^0}}{\sqrt{2\pi R} (\nu_m^0 - (\frac{\ell}{R} + A)^2)} \left(\sin 2\pi RA + i \cos 2\pi R\sqrt{\nu_m^0} \right) \quad (5.17)$$

for $\alpha_0 \neq 0, \alpha_1 = 0$ with $m \in \mathbb{N} \setminus \{0\}, \ell \in \mathbb{Z}$. Note that in the latter case one has to substitute the *ordered* basis $\{\phi_n\}_{n=1}^\infty$ (together with the corresponding eigenvalues) into Ansatz (4.6) to make the numerical procedure of cut-off approximations convergent.

Unless $\alpha_1 < 0$ we have to exclude here the possibility $2RA \in 2\mathbb{N}+1$ again (*cf.*, *e.g.*, (4.2)). Next we can restrict our attention only to the situation when $2RA \in [0, 1) \cup (1, 2)$ because A appears in the overlap integrals (5.16), (5.17) and in the spectral condition (5.12) as an argument of the periodic functions \sin, \cos ; the integrals and the transverse eigenvalues are the only quantities which affect the equations (4.9) and (4.18).

In fact, we can take $2RA$ from $[0, 1)$ only because the replacement $2RA \mapsto 2 - 2RA$ in (5.16) and (5.17) (the spectral condition (5.12) does not change at all) is equivalent to the exchange $A \mapsto -A$ which coincides with the conjugation of Hamiltonian (5.6). It is well known fact that such an operator has the same energies while the corresponding eigenfunctions are given by a simple conjugation.

As an example, the evolution of the quantum probability flow w.r.t. α_0 is illustrated on Figure 10.

References

- [AGHH] S. Albeverio, F. Gesztesy, R. Høegh-Krohn, and H. Holden, *Solvable models in quantum mechanics*, Springer, Heidelberg, 1988.
- [AS] M. Andrews, C.M. Savage: *Bound states in two-dimensional nonuniform waveguides*, Phys. Rev. **A50** (1994), 4535–4537.
- [BGRS] W. Bulla, F. Gesztesy, W. Renger, B. Simon: *Weakly coupled bound states in quantum waveguides*, Proc. Am. Math. Soc. **125** (1997), 1487–1495.
- [DE] P. Duclos and P. Exner, *Curvature-induced bound states in quantum waveguides in two and three dimensions*, Rev. Math. Phys. **7** (1995), 73–102.
- [DEM] P. Duclos, P. Exner, B. Meller: *Exponential bounds on curvature-induced resonances in a two-dimensional Dirichlet tube*, Helv. Phys. Acta **71** (1998), 133–162.
- [DEŠ] P. Duclos, P. Exner, P. Šťovíček: *Curvature-induced resonances in a two-dimensional Dirichlet tube*, Ann. Inst. H. Poincaré **62** (1995), 81–101.
- [EK] P. Exner, D. Krejčířík: *Waveguides coupled through a semitransparent barrier: the weak-coupling behaviour*, in preparation.
- [EŠ] P. Exner and P. Šeba, *Bound states in curved quantum waveguides*, J. Math. Phys. **30** (1989), 2574–2580.
- [EŠTV] P. Exner, P. Šeba, M. Tater, and D. Vaněk, *Bound states and scattering in quantum waveguides coupled laterally through a boundary window*, J. Math. Phys. **37** (1996), 4867–4887.

- [EV1] P. Exner, S.A. Vugalter: *Bound states in a locally deformed waveguide: the critical case*, Lett. Math. Phys. **39** (1997), 57–69.
- [EV2] P. Exner and S. A. Vugalter, *Asymptotic estimates for bound states in quantum waveguides coupled laterally through a narrow window*, Ann. Inst. H. Poincaré **65** (1996), 109–123.
- [EV3] P. Exner and S. A. Vugalter, *Bound-state asymptotic estimates for window-coupled Dirichlet strips and layers*, J. Phys. A: Math. Gen. **30** (1997), 7863–7878.
- [GJ] J. Goldstone and R. L. Jaffe, *Bound states in twisting tubes*, Phys. Rev. **B 45** (1992), 14100–14107.
- [HTW] Y. Hirayama, Y. Tokura, A.D. Wieck, S. Koch, R.J. Haug, K. von Klitzing, K. Ploog: *Transport characteristics of a window-coupled in-plane-gated wire system*, Phys. Rev. **B48** (1993), 7991–7998.
- [Ku] Ch. Kunze: *Leaky and mutually coupled quantum wires*, Phys. Rev. **B48** (1993), 14338–14346.
- [Po] A.N. Popov: *On the existence of eigenoscillations of a resonator open to a waveguide*, Sov. J. Tech. Phys. **56** (1986), 1916–1922.
- [Pop] I.Yu. Popov: *Asymptotics of bound states for laterally coupled waveguides*, Rep. Math. Phys., to appear
- [RB] W. Renger, W. Bulla: *Existence of bound states in quantum waveguides under weak conditions*, Lett. Math. Phys. **35** (1995), 1–12.
- [SRW] R.L. Schult, D.G. Ravenhall, H.W. Wyld: *Quantum bound state in classically unbound system of crossed wires*, Phys. Rev. **B39**, (1989), 5476–5479.

List of Figures

1	Double waveguide with a δ barrier.	2
2	Bound state energies <i>vs.</i> the halfwidth \tilde{a} in the symmetric case for $\tilde{\alpha}_0 = 10^5$ (\square), 50 (\circ), 10 ($*$), 5 (\times), 2 ($+$), 0.5 (\bullet).	9
3	Ground-state eigenfunctions in the symmetric case for $a/d = 0.15$	10
4	Narrow-window asymptotic power and coefficient as functions of α_0	11
5	The eigenfunction of the second excited state for $\nu = 1$, $a/d = 5$, $\alpha_1 = 0$	12
6	The maximum bending of nodal lines of third eigenfunctions in the symmetric case as a function of α_0 for a fixed window width.	13
7	Right-left conductivity as a function of k , d_2 for $d = \pi$, $a = 2\pi$, $\alpha_1 = 0$	14
8	Probability flow patterns for $\tilde{k} = 1.745$ and $\alpha_1 = 0$ in the symmetric situation. . .	15
9	Cylindrical strip with a δ barrier in axial magnetic field.	16
10	The quantum probability flow on the cylinder surface for $\tilde{A} = 0.5$, $\tilde{k} = 1.705$ and $\tilde{\alpha}_1 = 10^{-5}$	18